Available online at www.sciencedirect.com
ScienceDirect
Journal of Molecular Graphics and Modelling 25 (2007) 794–800
Journal of Molecular Graphics and Modelling
www.elsevier.com/locate/JMGM

# Shape effects on the activity of synthetic major-groove binding ligands

Syma Khalid [1], Michael J. Hannon [2], Alison Rodger, P. Mark Rodger *

*Department of Chemistry, University of Warwick, Coventry CV4 7AL, UK*

Received 17 February 2006; received in revised form 5 July 2006; accepted 5 July 2006
Available online 11 July 2006

**Abstract**

In this work we present the results of a molecular simulation study of two different tetracationic bis iron(II) supramolecular cylinders interacting with DNA. One cylinder has been shown to bind in the major groove of DNA and to induce dramatic coiling of the DNA; the second is a derivative of the first, with additional methyl groups attached so as to give a larger cylinder-radius. The simulations show that both cylinders bind strongly to the major groove of the DNA, and induce complex structural changes in A–T rich regions. Whereas the parent cylinder tends to bind along the major groove, the derivatised cylinder tends to twist so that only one end remains within the major groove. Both G–C rich and A–T rich binding sites for the derivatised cylinder are discussed.


*Keywords:* DNA; Major groove; Molecular dynamics; DNA coiling; Macromolecular cylinder

## 1. Introduction

Advances in chemical biology over the last decade have meant that developing methods to control gene expression has become a major research goal [1–4]. One of the ways being considered for this is to use ligands that bind non-covalently to specific sequences of DNA, thereby either activating or suppressing transcription. In this, researchers are seeking to develop compounds that will mimic biological systems, where such control is often exerted through proteins that bind non-covalently and sequence-specifically in the major groove of DNA [5–7]. Recently, the first step towards this aim has been achieved with the synthesis of a dimetallic supramolecular cylinder (**1**, Fig. 1) that has been shown to bind very strongly, and non-covalently, to the major groove of DNA and to induce a very large degree of binding in the duplex [8,9]: flow linear dichroism studies indicate this cylinder bends DNA by as much as 40°–60° per bound molecule [10], whereas known bending agents such as cobalt ammines generate just 2°–5° bend per bound molecule [11].

In a recent molecular simulation study of the influence of **1** on DNA [12] the authors showed that the DNA response is surprisingly independent of the electrostatic interactions between the DNA and the cylinder.[3] In particular, a neutralised version of **1** was found to bend the DNA at least as strongly as did the parent, tetracationic, cylinder. This suggests that the biological effect of the cylinder may depend strongly on its detailed shape, as expressed through the shorter ranged van der Waals forces. It is therefore of interest to examine how sensitive the DNA/cylinder complex is to derivatisation of the cylinder. In this paper we report the results of a comparative molecular dynamics (MD) simulation study of the parent cylinder (**1**) and a hexamethylated derivative (**2**, Fig. 1) binding to the major groove of a DNA dodecamer; both cylinders were used in the M enantiomeric form. The choice of methylation site follows from our experimental and modelling deductions about the effect of this position on the interaction of the cylinders with cellulose [13].

## 2. Computational methods

Molecular simulations were carried out using the same protocol and potentials as were used in our previous study [12].

* Corresponding author.
*E-mail address:* p.m.rodger@warwick.ac.uk (P.M. Rodger).
[1] Current address: Department of Biochemistry, University of Oxford, South Parks Road, Oxford OX1 3QU, UK.
[2] Current address: School of Chemistry, University of Birmingham, Birmingham B15 2TT, UK.

[3] Because of the overlap of coordination chemistry and biological chemistry in this paper, we shall avoid the use of the term ''ligand'', and shall instead refer to the macromolecular cylinder simply as ''cylinder''.

1093-3263/$ – see front matter 
doi:10.1016/j.jmgm.2006.07.004

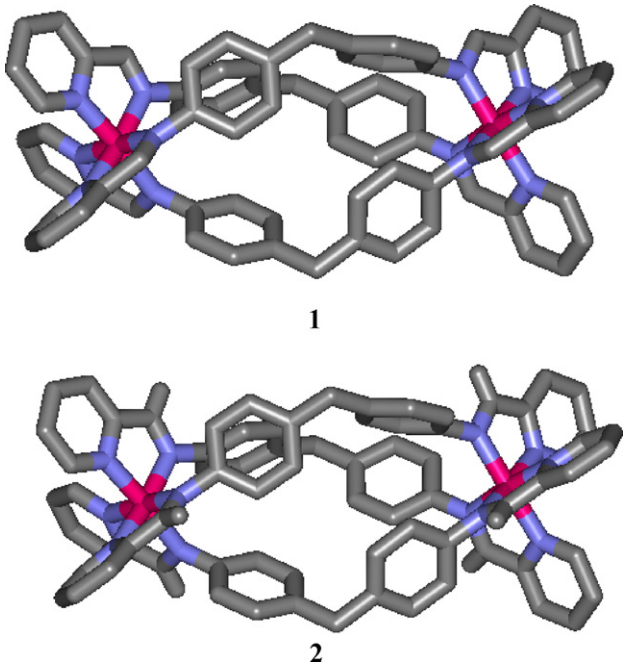


Fig. 1. The tetracationic supramolecular cylinder $[Fe_2(C_{25}H_{20}N_6)]^{4+}$ (**1**, denoted $C^{4+}$) and a derivative $[Fe_2(C_{31}H_{32}N_6)]^{4+}$, in which a methyl group has been added to each of the six imine carbon atoms (**2**, denoted $D^{4+}$). M enantiomers have been used in both cases. Colour key: $Fe^{II}$, pink; N, blue; C, grey; H atoms not shown.

Molecular dynamics (MD) simulations were used to simulate the response of a DNA dodecamer, d(CCCCCTTTTTCC)•d(GGAAAAAGGGGG) to the presence of either the supramolecular cylinder **1** ($C^{4+}$) or its derivative **2** ($D^{4+}$). A four-step protocol was used to achieve this:

(1) Potential binding sites were identified from high temperature MD simulations; the DNA duplex was immobilised, the cylinder treated as a rigid body, and the environment modelled as a continuum dielectric solvent but with explicit counterions. Configurations with favourable cylinder/DNA interaction energies were identified, and the energy optimised with respect to position of the cylinder (only). The resulting structure was used as the initial DNA/cylinder/counterion conformation for subsequent calculations. Manual docking was also used to check the validity of the binding sites found. Due to the accessibility of the cylinder to the DNA grooves, comprehensive identification of binding sites was possible without resorting to more sophisticated docking methods.
(2) The DNA/cylinder dimers were solvated with explicit water molecules.
(3) A series of six short equilibration MD simulations were performed in which the DNA was harmonically restrained to the canonical B-conformation (with force constants reducing from 100 to 1 kcal/mol/Å$^2$). In all other respects, the full intermolecular potentials were used for these calculations.
(4) Five nanosecond MD simulations were then performed on the fully atomistic system without any restraints. As with the previous study, the major dynamical response of the DNA was complete within about 1 ns. We report here the data for the first 3 ns so as to focus on the DNA response.

A number of alternative low energy conformations were examined and all found to involve major groove binding. Several of these were then carried forward into full solvated MD simulations following the protocol given above [14]. All such simulations exhibited a very similar DNA response to that reported herein – particularly with respect to the extent to which they bent the DNA, and the resultant stability of the DNA – and confirmed that the results of our simulations were not sensitive to variations in the initial binding site. These repeat simulations also proved our results to be robust with respect to the initial background ion distribution, since each configuration involved a very different, essentially random, initial arrangement of the sodium and chloride ions.

The cylinder was modelled using the CHARMM22 force-field [15], but with the $FeN_6$ sub-unit treated as a rigid body with geometry taken from the crystal structure [16]. The use of a rigid $FeN_6$ subunit obviates the need to develop either van der Waals or intra-molecular potentials for the $Fe^{II}$ centre, and the overall cylinder potential was found to give a good description of the crystal structure of **1** [14]. $Na^+$ and $Cl^-$ were modelled with CHARMM22 and water with TIP3P [17].

We have also chosen to model the DNA duplex using CHARMM22. While it is more usual to model DNA using the CHARMM27 force-field [18,19] we note that CHARMM27 was not designed for, nor fitted to, systems with strongly interacting macromolecules such as **1**. A comparison of these two force-fields for **1** bound to DNA was reported in our earlier study [12] and revealed that the CHARMM22 force-field does have some advantages over CHARMM27 when this highly charged cationic cylinder is bound to the major groove. In particular, whereas CHARMM27 underestimated the extent of bending and produced a stable B-DNA duplex, CHARMM22 predicted that $C^{4+}$ disrupted A–T base pairs adjacent to the cylinder binding site; similar disruption has since been confirmed in experimental crystal structures [20]. We have therefore used CHARMM22 to model the DNA interacting with **1** and **2** in this work.

Calculations were performed using DL_POLY [21]; the validity of using CHARMM force-fields within DL_POLY has been demonstrated previously [12,22]. Simulations were performed in the NVT ensemble (Hoover thermostat) with orthorhombic periodic boundary conditions and an EWALD treatment of the electrostatic interactions. Each system contained the DNA, cylinder, 3270 water molecules (TIP3P), 58 $Cl^-$ anions and 78 $Na^+$ cations in a 45 Å × 45 Å × 60 Å orthorhombic simulation cell. The resulting ionic strength ([NaCl] = 0.8 M) was chosen for consistency with our previous work [12] and is similar to that used in some other MD studies [23,24]. Analysis of the structural changes was performed with 3DNA [25] and of DNA-cylinder mobility using VMD [26].

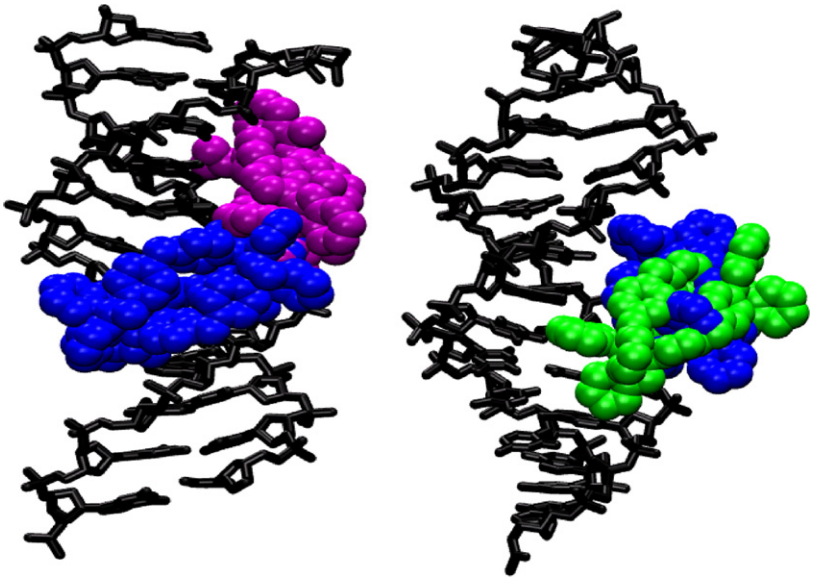

Fig. 2. DNA-cylinder starting geometries: $D_{AT}$ (blue), $D_{GC}$ (purple) and $C_{AT}$ (green); the DNA is the same in the left and right figures, but is viewed from different angles to provide a clear view of the binding sites.

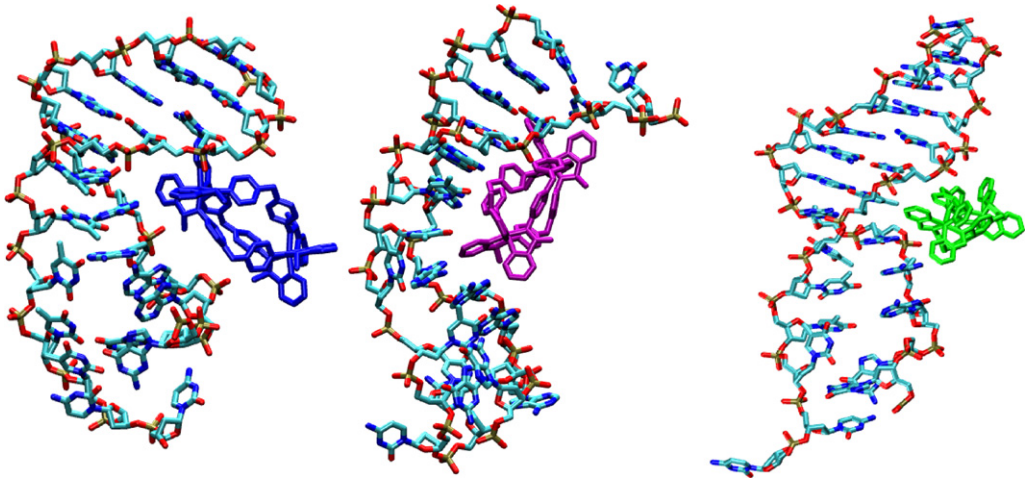

Fig. 3. DNA/cylinder configurations after 3 ns: DNA/$D_{AT}$ (left), DNA/$D_{GC}$ (middle) and DNA/$C_{AT}$ (right).

## 3. Results

MD simulations were performed using two different low-energy major groove binding sites obtained from the docking calculations for $D^{4+}$: one associated predominantly with the A–T tract (base pairs 5–9) and the other with the G–C region of the DNA (base pairs 2–6). These binding sites shall be denoted $D_{AT}$ and $D_{GC}$, respectively; the symbols will also be used to refer to the simulations initiated with these binding sites. The A–T binding site was found to be nearly coincident with that found [12] for $C^{4+}$ ($C_{AT}$, see Fig. 2). Note that the $C_{AT}$ binding site, in which the cylinder lies symmetrically between the two strands of the DNA spanning base pairs 6–10, is also consistent with the structure reported from NMR data [9].

Snapshots taken after 3 ns are shown in Fig. 3. A comparison of Figs. 2 and 3 provides a graphical overview of the DNA response to cylinder binding. Substantial DNA conformational changes were observed in all three cases, with curvature of the DNA backbone and disruption of the A–T base pairs, particularly below the location of the bound cylinder. After 3 ns $C_{AT}$ remained within the major groove, but the location was no longer symmetrical with respect to the two DNA strands: there was contact[4] between the cylinder and bases C5, A16 and A17 (i.e. associated with base pairs 5, 7 and 8). The behaviour of the derivatised cylinder, $D^{4+}$, provides a distinct contrast. For both $D_{AT}$ and $D_{GC}$ the cylinder initially lay in the major groove (contact with bases A16, A17 and A18 for $D_{AT}$, and C2, C3, G19, G20, G21 and G22 for $D_{GC}$); however, it twisted during the course of the simulations so that only one end of the cylinder remained in the groove by the end of the

[4] "Contact" has been defined to occur when at least one of the inter-group atom–atom distances is less than 3.5 Å.

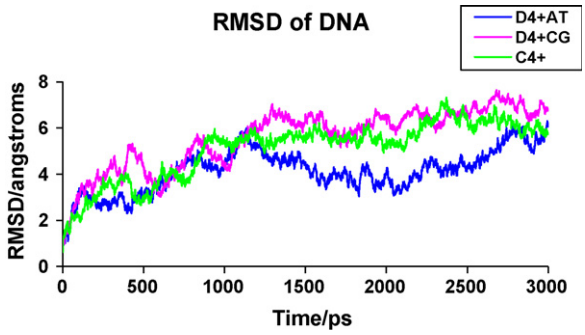


Fig. 4. Root mean square deviation of atomic positions from initial configuration; calculated using the middle 10 base pairs.

simulations. Close intermolecular distances, consistent with strong binding, were still present at the end of the simulation, with $D^{4+}$ associated with C3 and A18 at the end of the $D_{AT}$ simulation, but C5, A16, A17, A18, G19 and G20 for the end of the $D_{GC}$ simulation. In all three systems there were also strong interactions between the cylinder and the backbone, but whereas $C^{4+}$ interacted with both strands of the DNA, the $D^{4+}$ tended to interact with just one strand by the end of the simulation (phosphate groups 16, 18 and 19 for $D_{AT}$ and 17, 18, 19 for $D_{GC}$). It is intriguing to note that the two initial sites for $D^{4+}$ resulted in very similar cylinder/DNA interactions by the end of the simulation; this is consistent with the substantial reorientation of $D^{4+}$ already noted, and suggests that the larger size of $D^{4+}$ compared with $C^{4+}$ does not allow it to be constrained within specific major groove sites.

Substantial relaxation of the DNA in the presence of the cylinders is seen in each simulation, with root mean square deviations in the atomic positions in the middle ten base pairs growing to about 7 Å by 3 ns (Fig. 4). In part this was due to bending of the DNA around the cylinder, which is evident in all three systems (Fig. 3, and see discussion below), but is probably greatest and most localised with $D_{AT}$. However, considerable disruption of the DNA duplex was also seen in each system, particularly in the region of the A–T tract. Some indication of this is apparent in Fig. 3, but is much clearer in the analysis of the inter-nucleoside hydrogen bonding given in Table 1. Apart from some end-fraying in $C_{AT}$, the initial G–C tract (base pairs 1–5) is seen to be completely stable in all three systems. The A–T tract (base pairs 6–10), however, was disrupted in each simulation. This disruption was essentially complete where the cylinder was bound directly to the G–C tract, but a complex base-pair structure was observed when either cylinder was bound to the A–T tract. In these two cases, a series of base-pair mismatches were induced in the A–T rich region (indicated in bold in Table 1), which also appeared to help retain some of the original Watson-Crick base pairing (base pairs 6–19 and 7–18 for $D_{AT}$ and 6–19, 8–17 and 10–15 for $C_{AT}$). Although more base pairs appear to be retained in $C_{AT}$, there were in fact fewer hydrogen bonds and at longer distances in this system, and it was the $D_{AT}$ system that was more stable.

The structural changes induced in the A–T region by $C_{AT}$ and $D_{AT}$ was in fact both complex and dynamic, with multiple disruption, mismatch and reformation events being identified within the A–T base pairs. In the case of $C_{AT}$, the eighth (T8–A17), ninth (T9–A16) and tenth (T10–A15) base pairs were all seen to break and then reform over about 0.5–1.0 ns; in each case the reformed base pair remained stable for hundreds of picoseconds before subsequently being disrupted again. At least six separate mismatched pair formations (7A–17T three times, 8A–16T once and 10T–14G twice) were observed, with most of the mismatches lasting in excess of 200 ps. This dynamic behaviour was even richer for $D_{AT}$. For example, with

Table 1
Intra-base pair hydrogen bond distances for the average DNA calculated over the third nanosecond

| Base pairings | Length/Å | | | | | | | | |
|---|---|---|---|---|---|---|---|---|---|
| | DNA/$D_{AT}$ | | | DNA / $D_{GC}$ | | | DNA / $C_{AT}$ | | |
| | O2-N2/ O4-N6 | N3-N1 | N4-O6 | O2-N2/ O4-N6 | N3-N1 | N4-O6 | O2-N2/ O4-N6 | N3-N1 | N4-O6 |
| [1–24] C–G | 3.60 | 3.79 | 3.92 | 2.86 | 3.17 | 3.32 | | | |
| [2–23] C–G | 2.83 | 2.97 | 2.97 | 2.86 | 2.95 | 2.87 | 2.77 | 2.99 | 3.23 |
| [3–22] C–G | 2.89 | 2.98 | 2.91 | 2.87 | 2.98 | 2.91 | 2.84 | 2.90 | 2.78 |
| [4–21] C–G | 2.87 | 2.99 | 2.93 | 2.92 | 2.99 | 2.91 | 2.85 | 2.95 | 2.88 |
| [5–20] C–G | 2.88 | 3.01 | 2.96 | 2.81 | 2.90 | 2.84 | 2.94 | 2.99 | 2.88 |
| [6–19] T–A | 2.94 | 3.04 | | 2.85 | 3.35 | | 2.96 | 3.02 | |
| [7–18] T–A | 2.97 | 3.00 | | | | | **3.53** | **2.70** | |
| [8–17] T–A | **3.78** | | | | | | 3.38 | | |
| [9–16] T–A | **3.94** | | | | | | **3.34** | | |
| [10–15] T–A | **2.32** | **3.25** | | | | | 3.15 | | |
| [11–14] C–G | **3.26** | | | | | | | | |
| [12–13] C–G | | | | | | | | | |

The shaded boxes indicate the absence of a hydrogen bond, bold indicates hydrogen bonds between mismatched base pairs. Analysis was performed with 3DNA.

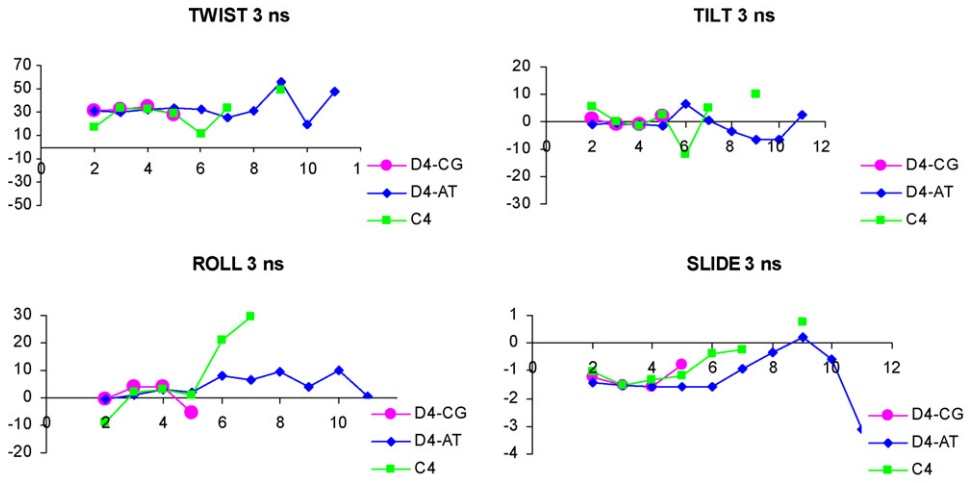


Fig. 5. Plots of the twist, tilt and roll inter-base pair angles and the slide inter-base pair distance for the DNA conformation averaged over the third nanosecond.

$D_{AT}$ the T8–A17 and T9–A16 step was observed to form a mismatched pair (T9–A17) on four separate occasions, only to reform the two original Watson-Crick base pairs on each occasion, before a non-Watson-Crick H-bond was formed in base pair T9–A16 at about 2 ns which then remained for the rest of the simulation. It is interesting to note that none of the reformation events were evident with $D_{GC}$, suggesting that these cylinders are much more effective in controlling A–T base pair behaviour than the more strongly hydrogen bound G–C pairs.

It was suggested above that the dramatic conformational changes in the DNA evident in Fig. 3 were not limited to the disruption of the base pairs, but also include bending of the DNA backbone. However, it is difficult to be definitive about this. The analysis of DNA curvature is usually performed in terms of the relative geometry of adjacent base pairs (slide distance and tilt, roll and twist angles), but such an analysis presupposes the presence of stable Watson-Crick base pairs within the duplex. It is not clear to what extent such an analysis is still meaningful in the presence of the deformations in the base pairings in the A–T tract noted above. Never-the-less, base pair geometrical parameters, as calculated with 3DNA, are presented in Fig. 5 for the three DNA/cylinder systems. Parameters have been calculated for the average DNA structure observed during the third nanosecond of each simulation. Given the stable base-pairings apparent in Table 1, we expect parameters for the first five steps to be reliable and unambiguous, although interpretations based on later steps (6–11) should be treated with some caution. We note that for the first five steps (base pairs C1–G24 through T6–A19), the geometric parameters show almost no variation between the first and third nanoseconds, and so only data for the third nanosecond are presented here.

The step parameters indicate that the DNA adopts a structure that is not consistent with the canonical form of either A or B-DNA. Slide values of less than −1 Å, usually indicative of A-DNA, were observed for the $D_{AT}$ and $D_{GC}$ simulations and values intermediate between those expected for A and B DNA

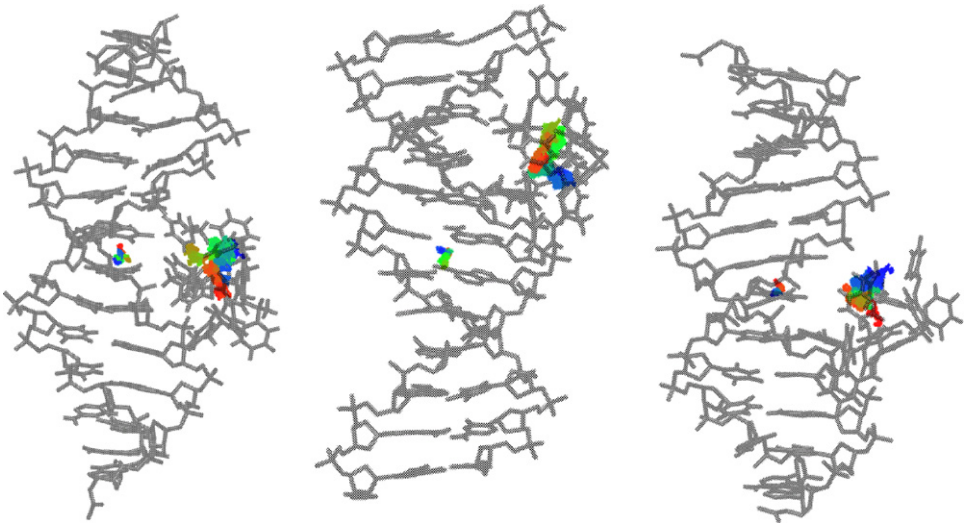

Fig. 6. $D_{AT}$ (left), $D_{GC}$ (middle) and $C_{AT}$ (right). A RGB colour scale is used to represent the time dependence of the centre of mass positions (red is at the beginning of the simulation, blue is at the end).

were found in $C_{AT}$. On the other hand, whereas the A form of DNA is usually associated with negative values for the roll angle, all three cylinders induced positive roll angles, as is more often associated with the B-form. The twist angles in all three simulations were intermediate between those expected for the A and B forms of DNA. We conclude that these cylinders do have a substantial effect on the DNA conformation, but that the nature of this effect is difficult to categorise in terms of canonical forms—particularly with the relatively short DNA strands (dodecamers) considered here. Simulations with longer segments of DNA are in progress.

Some interesting differences were also observed in the relative motion of the DNA and cylinder. Visual inspection of the three trajectories revealed substantial movement of the cylinder with respect to the DNA. As commented earlier, the $C_{AT}$ cylinder appears to remain within the major groove throughout the simulations, although one end is in closer contact with the DNA than the other by the end of the simulation, while the larger $D^{4+}$ twists much more prominently so that the cylinder lies only partially within the groove for much of the $D_{AT}$ and $D_{GC}$ trajectories.

We have used VMD [26] to monitor the time dependence of the centres of mass of the cylinder and the DNA, and also the displacement vector between the two centres of mass. Plots of the centre of mass trajectories are given in Fig. 6. In each of the three simulations there is a much greater spread in the distribution of the cylinder centre of mass compared with the DNA centre of mass. A convenient measure of this spread is to calculate the root mean square distance (RMSD) of the centre of mass from the centre (i.e. average) of its own trajectory. Values for this (averaged over the first 3 ns) are listed in Table 2. The RMSD for the cylinder is a factor of 3.2–3.4 larger than that for the DNA duplex. The mean square displacement can be expressed as a double integral of the velocity time correlation function, and so should show a linear dependence on $kT/m$, where $k$ is Boltzmann's constant, $T$ the temperature and $m$ is the molecular mass; thus the RMSD should scale with the square root of the molecular mass. The DNA dodecamer is 6.7 times heavier than the cylinder, which would correspond to a factor of 2.6 in the RMSDs. While these two factors are comparable, the observed value is significantly larger and so indicates some correlation in the motion—possibly because the rotation of the DNA is being superimposed on the cylinder motion through its binding to the major groove.

Table 2
Root mean square distance along a trajectory

| System | Root mean square distance from the origin (Å) | | |
|---|---|---|---|
| | DNA | Cylinder | Displacement |
| $C_{AT}$ | 0.40 | 1.36 | 1.75 |
| $D_{AT}$ | 0.70 | 2.26 | 2.96 |
| $D_{GC}$ | 0.59 | 1.91 | 2.49 |

The origin is taken as the geometric centre of the trajectory (defined by the time average $x$, $y$ and $z$ coordinates). This "displacement" refers to the vector from the DNA centre of mass to the cylinder centre of mass, and is again shifted so that the time average of this vector is taken as the origin.

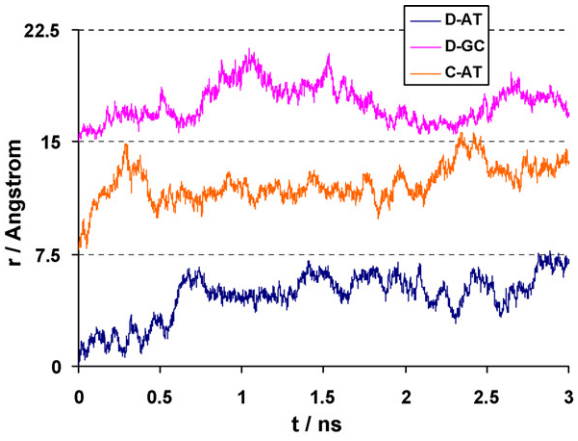


Fig. 7. Root mean square distance along a trajectory, as measured from the initial position. The trajectory is for the displacement vector from the DNA centre of mass to the cylinder (cylinder) centre of mass. Curves have been displaced vertically by 7.5 Å ($C_{AT}$) and 15 Å ($D_{GC}$) for clarity.

The motion of the cylinder relative to the DNA can be monitored in more detail by considering the distance:

$$d(t) = |\boldsymbol{r}_{DNA\rightarrow Cyl}(t) - \boldsymbol{r}_{DNA\rightarrow Cyl}(0)|$$

where $\boldsymbol{r}_{DNA\rightarrow Cyl}(t)$ is the vector from the DNA centre of mass to the cylinder centre of mass, both at time $t$. Plots of this quantity for the three systems are given in Fig. 7. All three systems show maximum distances of no more than 8 Å which, given the cylinders have molecular lengths of ca. 20 Å, may be explained by the reorientation of the cylinder so that it tends to point out from the major groove rather than lie within it. For both binding sites, the $D^{4+}$ cylinder shows an initial stable region, with little relative motion during the first 0.5 ns, followed by a relatively rapid rearrangement to a new position about 5 Å removed from its initial location. In contrast, the position of the $C^{4+}$ cylinder relaxes over the first 0.5 ns, albeit again finding a stable location about 5 Å from its initial position. Most intriguingly, the initial behaviour of $D_{AT}$ is oscillatory, with a period of about 100 ps, suggesting that while the initial binding site was only metastable, there was a substantial energy barrier to reorientation of the cylinder that was associated with relatively low-frequency collective motions in the DNA. Similar oscillations were not apparent with the smaller $C^{4+}$, which fitted into the major groove more easily; nor were they apparent when the binding was within the G–C tract. It is interesting to speculate whether such coupling to vibrational motion in the DNA may be the major-groove analogue of similar couplings seen for synergistic binding of Hoechst 33258 in the minor groove [27].

## 4. Conclusions

The simulations presented in this article reveal a rich and complex interaction between DNA and a new class of major groove binding ligands. These DNA-binding ligands are dimetallic macromolecular cylinders, such as **1** and **2**, and have dimensions (ca. 20 Å length and 10–12 Å radius) designed to match the major groove of DNA. As anticipated from our earlier work [12], the nature of the DNA response is sensitive to

the shape of the cylinder. In this work we have shown that a hexamethylated cylinder ($D^{4+}$, **2**), which has a significantly larger cylindrical radius than the parent compound ($C^{4+}$, **1**), binds to DNA in a mode that is not completely contained within the major groove. Instead, the cylinder reorients so that only one end occupies the major groove. Never-the-less, this larger cylinder still has a very strong effect on the conformation and stability of the DNA. Depending on the initial location of the binding site, the $D^{4+}$ may either disrupt A–T base pairs (when bound adjacent to them, but within a region rich in G–C pairs), or induce a complex set of base-pair mismatches when bound within the A–T-rich region. These mismatches were similar to those already reported for the parent cylinder, $C^{4+}$ [12], even though the binding geometries proved to be different with these two cylinders. We conclude that the dimetallic macromolecular cylinders do induce a response in the DNA that is dependent on the DNA sequence, and that the nature of this response can be varied by altering the shape of the cylinder.

## Acknowledgements

This work was supported by the EPSRC (S.K.; postgraduate studentship) and the European Union (MARCY RTN; HPRN-CT-2002-00175).

## References

[1] See, for example, J.M. Berg, J.L. Tymoczko, L. Stryer, Biochemistry, 5th ed., Freeman, New York, 2002.
[2] J.P. Baak, F.R. Path, M.A. Hermsen, G. Meijer, J. Schmidt, E.A. Janssen, Eur. J. Cancer 39 (2003) 1199–1215.
[3] C.F. Calkhoven, C. Muller, A. Leutz, Trends Mol. Med. 8 (2002) 577–583.
[4] L. Rogge, Arthritis Res. Ther. 5 (2003) 47–50.
[5] R.R. Sinden, DNA Structure and Function, Academic, London, 1994.
[6] R.E. Dickerson, Nucleic Acids Res. 26 (1998) 1906–1926.
[7] C. Branden, J. Tooze, Introduction to Protein Structure, 2nd ed., Garland, New York, 1999.
[8] I. Meistermann, A. Rodger, V. Moreno, M.J. Prieto, E. Moldrheim, E. Sletten, S. Khalid, P.M. Rodger, J. Peberdy, C.J. Isaac, M.J. Hannon, Proc. Natl. Acad. Sci. U.S.A. 99 (2002) 5069–5074.
[9] E. Molderheim, I. Meistermann, A. Rodger, M.J. Hannon, E. Sletten, J. Biol. Inorg. Chem. 7 (2002) 770–780.
[10] M.J. Hannon, V. Moreno, M.J. Prieto, E. Moldrheim, E. Sletten, I. Meistermann, C.J. Isaac, K.J. Sanders, A. Rodger, Angew. Chem. Int. Ed. Engl. 40 (2001) 879–884.
[11] A. Rodger, K.J. Sanders, M.J. Hannon, I. Meistermann, A. Parkinson, D.S. Vidler, I.S. Haworth, Chirality 12 (2000) 221–236.
[12] S. Khalid, M.J. Hannon, A. Rodger, P.M. Rodger, Chem. Eur. J. 12 (2006) 3493–3506.
[13] S. Khalid, P.M. Rodger, A. Rodger, J. Liq. Chromatogr. Rel. Technol. 28 (2005) 2995–3003.
[14] S. Khalid, PhD Thesis, University of Warwick, 2004.
[15] A.D. MacKerell Jr., D. Bashford, M. Bellot, R.L. Dunbrack Jr., J.D. Evanseck, M.J. Field, S. Fischer, J. Gao, H. Guo, S. Ha, D. Joseph-McCarthy, L. Kuchnir, K. Kuczera, F.T.K. Lau, C. Mattos, S. Michnik, T. Ngo, D.T. Nguyen, B. Prodhom, W.E. Reiher III, B. Roux, M. Schlenkrich, J.C. Smith, R. Stote, J. Straub, M. Watanabe, J. Wiorkiewicz-Kuczera, D. Yin, M. Karplus, J. Phys. Chem. B 102 (1998) 3586–3616.
[16] M.J. Hannon, C.L. Painting, J. Hamblin, A. Jackson, W. Errington, Chem. Commun. (1997) 1807–1808;
C.L. Painting, PhD Thesis, University of Warwick, 1999; I. Meistermann, L.J. Childs, F. Tuna, C.L. Painting, W. Errington, N.W. Alcock, A. Rodger, M.J. Hannon, in preparation.
[17] W.L. Jorgensen, J. Chandrasekhar, J.D. Madura, R.W. Impey, M.L. Klein, J. Chem. Phys. 79 (1983) 926–935.
[18] N. Foloppe, A.D. MacKerell Jr., J. Comp. Chem. 21 (2000) 86–104.
[19] A.D. MacKerell, N. Banavali, N. Foloppe, Biopolymers 56 (2000) 257–265.
[20] A. Oleksi, A.G. Blanco, R. Boer, I. Usón, J. Aymamí, A. Rodger, M.J. Hannon, M. Coll, Angew. Chem. Int. Ed. Engl. 45 (2006) 1227–1231.
[21] W. Smith, C.W. Yong, P.M. Rodger, Mol. Sim. 28 (2002) 385–471.
[22] M.A.S. Miguel, R. Marrington, P.M. Rodger, A. Rodger, C. Robinson, Eur. J. Biochem. 270 (2003) 3345–3352;
M.A.S. Miguel, P.M. Rodger, Phys. Chem. Chem. Phys. 5 (2003) 575–581;
R. Lukac, A.J. Clark, M.A.S. Miguel, A. Rodger, P.M. Rodger, J. Mol. Liq. 101 (2002) 261–272;
T. Astley, G.G. Birch, M.G.B. Drew, P.M. Rodger, J. Phys. Chem. A 103 (1999) 5080–5090.
[23] M. Feig, B.M. Pettitt, Biophys. J. 75 (1998) 134–149.
[24] N. Korolev, A.P. Lyubartsev, A. Laaksonen, L. Nordenskiöld, Biophys. J. 82 (2002) 2860–2875.
[25] X.J. Lu, W.K. Olson, Nucleic Acids Res. 31 (2003) 5108–5121.
[26] W. Humphrey, A. Dalke, K. Schulten, J. Mol. Graphics 14 (1996) 33–38.
[27] S.A. Harris, E. Gavathiotis, M.S. Searle, M. Orozco, C.A. Laughton, J. Am. Chem. Soc. 123 (2001) 12658–12663.